

Zooming on the emerging ionized regions of pPNe with ALMA

C. Sánchez Contreras¹, D. Tafoya², J. P. Fonfría¹, J. Alcolea³, A. Castro-Carrizo⁴,
and V. Bujarrabal³

¹ Centro de Astrobiología (CAB), CSIC-INTA. Postal address: ESAC, Camino Bajo del Castillo s/n, E-28692, Villanueva de la Cañada, Madrid, Spain.

² Department of Space, Earth and Environment, Chalmers University of Technology, Onsala Space Observatory, 439 92 Onsala, Sweden.

³ Observatorio Astronómico Nacional (IGN), Alfonso XII No 3, 28014 Madrid, Spain.

⁴ Institut de Radioastronomie Millimétrique, 300 rue de la Piscine, 38406 Saint Martin d'Herès, France.

Abstract. We report on recent results from our successful and pioneering observational program with ALMA to study emerging ultracompact HII regions of pre-planetary nebulae (pPNe) using mm-wavelength recombination lines (mRRLs) as new optimal tracers. We focus on our study of two poster-child pPNe, namely, M2-9 and CRL 618. We reveal the structure and kinematics of the enigmatic inner nebular regions of these objects with an unprecedented angular resolution down to 20-30 mas (~ 15 -30 AU linear scales). For both targets, the ionized central regions are elongated along the main symmetry axis of the large-scale nebulae, consistent with bipolar winds, and show notable axial velocity gradients with expansion velocities of up to ~ 100 km s⁻¹. The intensity and width of the H30 α profiles are found to be time variable, denoting changes on scales of a few years of the physical properties and kinematics of the present-day post-AGB ejections. Our ongoing analysis involves 3D, non-LTE radiative transfer modeling of the mRRLs and free-free continuum emission. This approach allows us to provide an exceptionally detailed description of the physical conditions in the innermost layers of these well known pPNe.

Keywords. stars: AGB and post-AGB, circumstellar matter, stars: mass-loss, stars: winds, outflows, planetary nebulae: individual (M2-9, CRL 618).

1. Introduction

Previous studies of pPNe and young PNe (yPNe) suggest that multiple lobes and high velocities may result from collimated fast winds (CFWs or “jets”) interacting with slowly expanding circumstellar envelopes formed during the previous AGB phase (see e.g. Balick & Frank 2002, for a comprehensive review). However, directly characterizing post-AGB jets and their launch regions within a few hundred astronomical units is challenging due to their small angular sizes and significant obscuration caused by optically thick circumstellar dust shells or disks. A recent pilot study using millimeter radio recombination lines (mRRLs) in a sample of pPNe/yPNe observed with the IRAM-30 m radiotelescope shows that mRRLs are optimal tracers to probe very deep ionized nebular regions ($\lesssim 150$ au), taking us closer to the sites where CFWs are launched and facilitating the measurement of the mass-loss rate of ongoing post-AGB ejections (Sánchez Contreras et al. 2017, hereafter CSC+17). CSC+17 reported the detection of mRRLs in three (out of eight) objects within their sample: MWC 922, M2-9, and CRL 618, resulting in the first characterization of the spatio-kinematic structure and physical conditions of their central ionized regions.

For M2-9 and CRL 618, the data revealed the existence of young ($\lesssim 15$ -20 yr) bipolar outflows characterized by moderate average velocities (of a few tens of km s⁻¹) and relatively high mass-loss rates ($\approx 10^{-7}$ - $10^{-6} M_{\odot}$ yr⁻¹). In the case of MWC 922, an IR excess B[e]-type

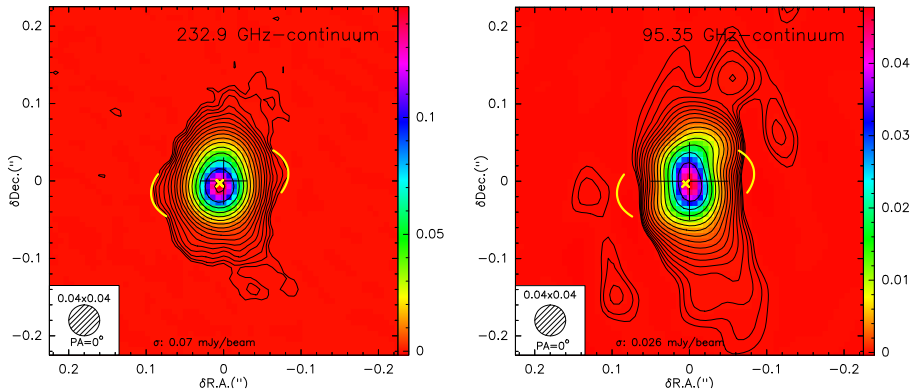


Figure 1. ALMA continuum emission maps of M2-9 at 232.9 GHz (left) and 95.4 GHz (right) using a circular restoring beam with half power beam width of $\text{HPBW}=0.04''$. The level contours are $(3\sigma) \times 1.5^{(i-1)}$ Jy beam $^{-1}$, $i=1,2,3\dots$. The central cross marks the 3 mm continuum surface brightness peak at coordinates J2000 R.A.= $17^{\text{h}}05^{\text{m}}37.96679$ and Dec.= $-10^{\circ}08'32.65$ (J2000). The yellow arcs, centered at the small yellow cross, represent the broad-waist structure, plausibly a dust disc.

star surrounded by a large-scale reflection nebulosity displaying a remarkable X-shape morphology, the line profiles suggested the presence of both a rotating disk and a wind. Through a subsequent ALMA study, Sánchez Contreras et al. (2019) provided evidence for a spatially resolved, nearly edge-on rotating disk and also uncovered a fast ($\sim 100 \text{ km s}^{-1}$) bipolar wind perpendicular to the disk, which was found to rotate in tandem with the disk itself.

This contribution outlines our ongoing ALMA-based study of the emerging compact ionized region at the cores of M2-9 and CRL 618.

2. Observations

The observations of M2-9 and CRL 618 were conducted using the ALMA 12-m array as part of projects 2016.1.00161.S and 2017.1.00376.S. The observations were carried out in Band 3 (3 mm) and Band 6 (1 mm), with a total of twelve different spectral windows (SPWs) dedicated to mapping the emission of various mRRLs (and CO lines) as well as the continuum. Observations were conducted in October and November 2017 using 45-50 antennas, with baselines ranging from 41.4 m to 16.2 km for Band 3, and from 41.4 m to 14.9 km for Band 6. The maximum recoverable scale (MRS) of the observations is $\sim 0.8''$ and $\sim 0.7''$ at 3 and 1 mm, respectively. Full details on the observations and imaging techniques for M2-9 and CRL 618 can be found in Sánchez Contreras et al. and Fonfría et al., in preparation, respectively. The final mRRLs cubes and continuum maps presented here have angular resolution of $\sim 40\text{-}60 \text{ mas}$ at 1 mm and $\sim 70\text{-}90 \text{ mas}$ at 3 mm.

3. M2-9 or “The Butterfly Nebula”

M2-9 is a very well-documented yPNe candidate that has gathered significant attention in the existing literature (e.g. Kwok et al. 1985; Corradi et al. 2011; Castro-Carrizo et al. 2012, 2017; Sánchez Contreras et al. 2017; Balick et al. 2018, and references therein). It has prominent large-scale lobes (oriented along the NS direction) with a dominant expansive kinematics. Indirect, yet compelling evidence suggests that M2-9 hosts a binary system with an orbital period of $\sim 90 \text{ yr}$, although the nature of this binary remains unknown. The extended lobes display observable radio-continuum free-free emission, contributing to a nearly flat spectral energy distribution at centimeter wavelengths. Additionally, a compact ($\lesssim 0.2''$) region at

the core emits radio-continuum, inferred to be an ionized wind based on the spectral index ($S_\nu \propto \nu^{(0.6-0.8)}$), which has been mapped using ALMA as part of this project.

The distance to M2-9 is highly uncertain, with values spanning from 50 pc to 3 kpc in the literature. The two most accepted values are $d=1.3$ kpc (Corradi et al. 2011) and $d=650$ pc (Castro-Carrizo et al. 2012) from the analysis of proper motions and other nebular properties at optical and mm wavelengths, respectively. We adopt a value of $d=650$ pc, which allows direct comparison with the study by CSC+17.

3.1. An ionized bent jet surrounded by a circumbinary disk

The ALMA continuum maps at 1 and 3 mm (Fig. 1), show an elongated structure that resembles what is seen at longer wavelengths. At 3 mm, we discern a C-shaped curvature similar to that observed in 2015 in the VLA 7 mm maps (de la Fuente et al. 2022) consistent with a bent collimated wind or jet emerging from the core. This wind has dimensions of $0''.4 \times 0''.13$ (260×85 au at $d=650$ pc) at 3 mm. We measure a spectral index of the continuum of $S_\nu \propto \nu^{0.92 \pm 0.10}$, which suggests predominantly free-free emission from the ionized jet, with a minor contribution from dust.

There are some differences between the 1 mm and 3 mm maps that partly arise from the frequency-dependence of the free-free continuum optical depth and from the increased contribution of thermal emission from dust to the continuum at shorter wavelengths. In particular, the 1 mm maps show a broad-waist of emission, absent at 3 mm and in the mRRLs maps, which very likely represents a dusty equatorial disk (with a radius of ~ 50 au) surrounding the ionized jet. This mm-continuum disk is probably the counterpart of the compact, dust disk known to exist at the core of M2-9 based on mid-infrared observations (Lykou et al. 2011).

Further support for the existence of an equatorial disk around the ionized jet comes from our observation of CO compact absorption at the center (not shown). Notably, this absorption is slightly offset to the north (by $\sim 0''.012$). Considering the system's inclination, with the north lobe oriented at an angle of $i \sim 17^\circ$ away from the plane of the sky, this offset is in line with the absorption of the background free-free continuum (from the ionized core) occurring by the front part of an equatorial disk. The CO absorption feature is redshifted by ~ 6 km s $^{-1}$ from the centroid of the mRRLs, which is most likely due to infall motions from the inner regions of the circumbinary disk.

3.2. Kinematics of the ionized jet

As shown in Fig. 2, the H30 α and H39 α line emission span a wide velocity range of ~ 140 km s $^{-1}$, sharing a similar extent and morphology with the mm continuum emission (with the exception of the broad waist at 1 mm). The comparison between the ALMA line profiles (integrated over the emitting area) with those obtained 2 years earlier with the IRAM-30 m antenna (CSC+17) shows that the lines are now more intense and broader, implying changes of in the wind properties over yearly time scales.

The ionized jet's kinematics can be examined using the moment-1 maps and position-velocity diagrams. We observe a global expansion indicated by an overall velocity gradient along the nebula's symmetry axis (PA=0 $^\circ$). The velocity gradient suggests very short kinematical ages of less than approximately one year, consistent with the observed changes in the line profiles over the course of a year. Additionally, we note a slight velocity gradient perpendicular to the lobes, which is evident in the sloping (non-horizontal) isovelocity contours in the momentum-1 map, tentatively suggesting jet rotation. The axial position-velocity diagrams display a distinctive S-shape, showing maximum line widths at two compact regions located diametrically opposed along the axis (at offsets of ~ 20 -30 mas), indicating either rapid/abrupt wind acceleration or shocks at these compact regions (referred to as *HV spots*).

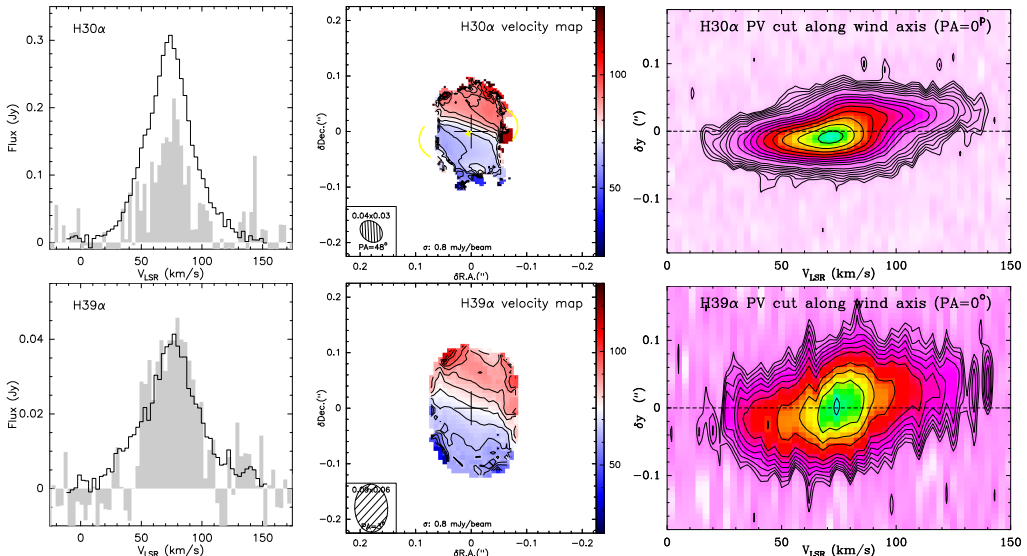


Figure 2. Summary of ALMA data of the H30 α (top) and H39 α (bottom) recombination lines. Left: Integrated line spectrum obtained with ALMA (black lines) and with the IRAM-30 m antenna (grey histogram, CSC+17). Middle: First moment map. Contours going from $V_{\text{LSR}}=45$ to 115 km s^{-1} by 5 km s^{-1} . The wedge indicates the V_{LSR} -color relationship. Right: Position velocity cuts through the center along the wind axis ($\text{PA}=0^\circ$). Levels are $2.5 \times (1.3)^{(i-1)}$ for H30 α and $1.5 \times (1.3)^{(i-1)}$ for H39 α with $i=1,2,3...$

3.3. Non-LTE radiative transfer modeling

For a comprehensive analysis of the spatio-kinematics and physical conditions of the ionized jet, we are currently conducting radiative transfer modeling using the co3Ral code developed by co-I D. Tafuya (Sánchez Contreras et al. in prep.). Although the modeling is ongoing, it appears that a wind with a non-uniform density structure is necessary to account for the observations. Notably, the HVspots are well depicted by two regions of high-density and high-velocity, resembling the shock-compressed bipolar structure proposed by Livio & Soker (2001) in their model for M2-9, which is based on the interaction of a tenuous companion-launched jet and the dense primary star’s wind. We find an average electron temperature of $\sim 15000 \text{ K}$ and electron densities ranging from $n_e \approx 10^6$ to 10^9 cm^{-3} . The average mass-loss rate of the ionized wind is deduced to be of $\dot{M} \approx 10^{-7} M_\odot \text{ yr}^{-1}$.

4. CRL 618 or “The Westbrook Nebula”

CRL 618 is a well-studied pPN exhibiting a complex and intricate multipolar structure, including fast outflows reaching expansion velocities of up to $\sim 200 \text{ km s}^{-1}$ and predominantly oriented in the east-west direction (e.g. Cernicharo et al. 1989; Sánchez Contreras et al. 2002, 2004; Riera et al. 2014). Compared with M2-9, CRL 618 has a younger and denser envelope, with the majority of its mass existing in the form of molecular gas (Sánchez Contreras & Sahai 2004; Pardo et al. 2007). A small fraction of material at its core gets ionized by a central B-type star, resulting in the emission of free-free continuum radiation and mRRLs (Kwok & Feldman 1981; Martín-Pintado et al. 1988; Tafuya et al. 2013). These mRRLs were initially observed by Martín-Pintado et al. (1988) and revisited by us in 2015 using the IRAM-30 m antenna (CSC+17), uncovering significant changes in their profiles and confirming ongoing fluctuations in free-free continuum emission over the past few decades.

We observed with ALMA the central ionized region of CRL 618 in 2017 within projects 2016.1.00161.S and 2017.1.00376.S. Regrettably, in this case, the 3 mm data failed the quality

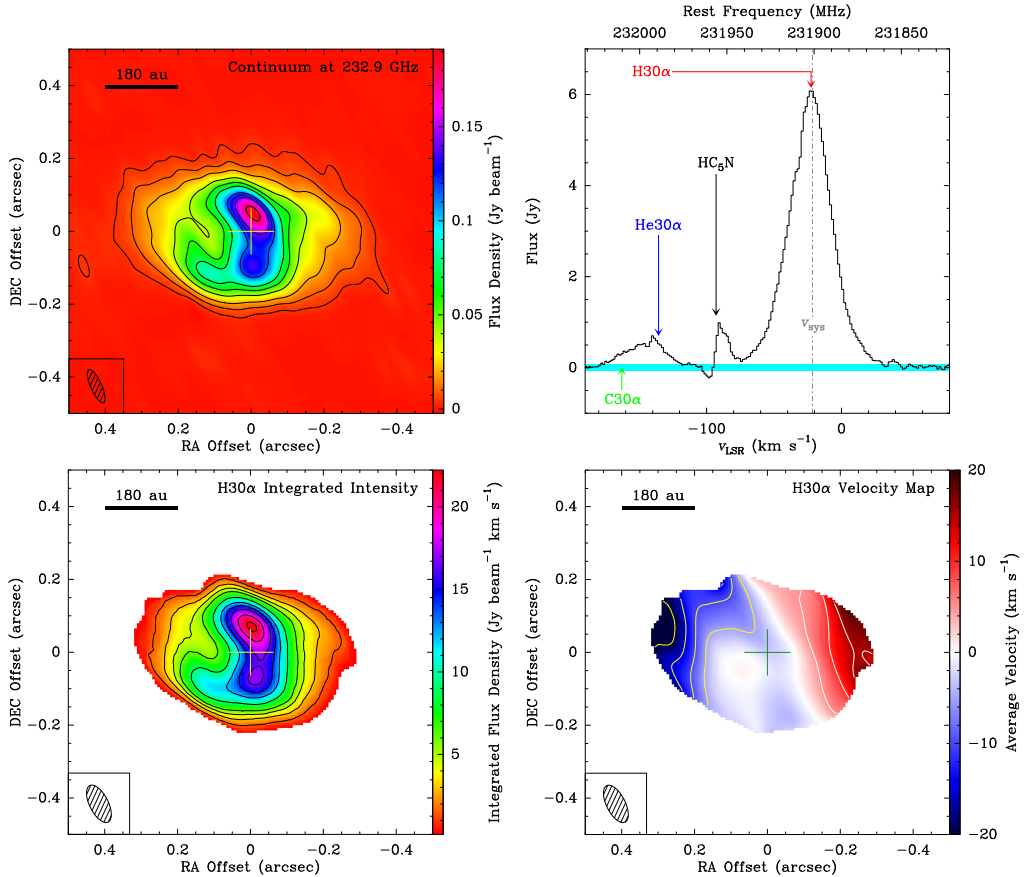


Figure 3. Summary of ALMA data for CRL 618. Top-left: Continuum emission map at 232.9 GHz. Top-right: Spectrum of H30 α integrated within the emitting area (other lines are also labeled). Bottom: Zeroth and first moment maps (left and right, respectively) of H30 α . The ellipse at the bottom-left corner of the maps represents the HPBW. The central cross marks the coordinates of the tracking center at R.A.= 04^h42^m53^s.583 and Dec.= 36°06′53″.34 (J2000).

assessment, leaving us only with the band 6 data (Fig. 3). Similarly to M2-9, the 1 mm continuum emission exhibits an elongation aligned with the main nebula axis, mirroring patterns observed at cm wavelengths, albeit on a smaller scale due to the lower opacity of the free-free continuum at mm-wavelengths. The brightness distribution is non-uniform and suggests a hollow cylindrical geometry, with inner and outer radius of ~ 70 and 110 au, respectively, with a dense equatorial zone.

The H30 α line profile exhibits broad wings, implying gas movements at speeds of ~ 70 –100 km/s within the cylindrical shell emitting the free-free continuum. The velocity map reveals a gradient along the east-west direction, i.e., the nebula main symmetry axis, indicating expansion and resulting in kinematical ages of just a few years. Despite the seemingly smooth appearance of the velocity map, a closer examination of the position-velocity diagrams indicates underlying complexity that we are currently investigating. For instance, the velocity field might encompass radial and axial expansions in varying proportions for the equator and the lobes. Additionally, we have noticed potential asymmetries in the geometry, such as the west lobe appearing shorter, and the cylindrical shell possibly being incomplete. We are currently exploring these and other intricacies using a 3D non-LTE radiative transfer model. This

effort aims to provide the most comprehensive characterization to date of the central regions, within ~ 300 au, of this iconic object.

5. Concluding remarks

In this presentation, we underscore the significance of mRRLs in probing the enigmatic central ionized regions of pPNe/yPNe. These lines offer a unique opportunity to closely investigate the jet engine and estimate the mass-loss rate of the ongoing ejections.

In conjunction with the previously published results from our ALMA project on MWC 922 (Sánchez Contreras et al. 2019), the current analysis of our ALMA mRRL emission maps of M2-9 and CRL 618 is delivering a comprehensive and detailed account of the structure, kinematics, and physical conditions in the central regions of pPNe. We are observing diverse properties of the ionized central regions in the three targets observed within our project, emphasizing the need for additional similar observations to gain meaningful statistical insights and advance our understanding of the development of nebular asymmetries and rapid outflows in these late evolutionary stages of low-to-intermediate mass stars.

We acknowledge funding from the Spanish MCIN/AEI/10.13039/501100011033 (projects PID2019-105203GB-C22 and PID2019-105203GB-C21). This paper makes use of the following ALMA data: ADS/JAO.ALMA#2016.1.00161.S and ADS/JAO.ALMA#2017.1.00376.S. ALMA is a partnership of ESO (representing its member states), NSF (USA) and NINS (Japan), together with NRC (Canada), MOST and ASIAA (Taiwan), and KASI (Republic of Korea), in cooperation with the Republic of Chile. The Joint ALMA Observatory is operated by ESO, AUI/NRAO and NAOJ.

References

- Balick, B., & Frank, A. 2002, *ARA&A*, 40, 439
- Balick, B., Frank, A., Liu, B., et al. 2018, *ApJ*, 853, 168.
- Castro-Carrizo, A., Neri, R., Bujarrabal, V., et al. 2012, *A&A*, 545, A1
- Castro-Carrizo, A., Bujarrabal, V., Neri, R., et al. 2017, *A&A*, 600, A4.
- Cernicharo, J., Guelin, M., Martín-Pintado, J., et al. 1989, *A&A* 222, L1
- Corradi, R. L. M., Balick, B., & Santander-García, M. 2011, *A&A*, 529, A43.
- de la Fuente, E., Trinidad, M. A., Tafuya, D., et al. 2022, *PASJ* 74, 594.
- Kwok, S. & Feldman, P. A. 1981, *ApJL* 247, L67.
- Kwok, S., Purton, C. R., Matthews, H. E., & Spoelstra, T. A. T. 1985, *A&A*, 144, 321
- Lim, J., & Kwok, S. 2000, *Asymmetrical Planetary Nebulae II: From Origins to Microstructures*, 199, 259
- Lim, J., & Kwok, S. 2003, *Symbiotic Stars Probing Stellar Evolution*, 303, 437
- Livio, M. & Soker, N. 2001, *ApJ* 552, 685.
- Lykou, F., Chesneau, O., Zijlstra, A. A., et al. 2011, *A&A*, 527, A105.
- Martín-Pintado, J., Bujarrabal, V., Bachiller, R., et al. 1988, *A&A* 197, L15
- Pardo, J. R., Cernicharo, J., Goicoechea, J. R., et al. 2007, *ApJ*, 661, 250.
- Riera, A., Velázquez, P. F., Raga, A. C., et al. 2014, *A&A* 561, A145.
- Sánchez Contreras, C., Bujarrabal, V., Castro-Carrizo, A., et al. 2004, *ApJ*, 617, 1142.
- Sánchez Contreras, C. & Sahai, R. 2004, *ApJ*, 602, 960.
- Sánchez Contreras, C., Sahai, R., & Gil de Paz, A. 2002, *ApJ*, 578, 269.
- Sánchez Contreras, C., Báez-Rubio, A., Alcolea, J., et al. 2017, *A&A*, 603, A67.
- Sánchez Contreras, C., Báez-Rubio, A., Alcolea, J., et al. 2019, *A&A*, 629, A136.
- Smith, N. & Gehrz, R. D. 2005, *AJ*, 129, 969.
- Schwarz, H. E., Aspin, C., Corradi, R. L. M., et al. 1997, *A&A*, 319, 267
- Tafuya, D., Loinard, L., Fonfría, J. P., et al. 2013, *A&A* 556, A35.